UNDERSTANDING THE ROLE OF ION FLUX IN SOLAR WIND SPACE WEATHERING: LOW FLUX H^+ AND HE^+ IRRADIATION OF THE MURCHISON METEORITE. D. L. Laczniak[1], M. S. Thompson[1], R. Christoffersen[2], C. A. Dukes[3], R. V. Morris[4], and L. P. Keller[4]. [1]Earth, Atmospheric, and Planetary Sciences Department, Purdue University, West Lafayette, IN, 47907 (dlacznia@purdue.edu), [2]Jacobs, NASA Johnson Space Center, Mail Code XI3, Houston, TX 77058, [3]Laboratory for Astrophysics and Surface Physics, University of Virginia, Charlottesville, VA, 22904, [4]NASA Johnson Space Center, Mail Code X13, Houston, TX 77058.

Introduction: Solar wind space weathering creates ion-damaged rims in the uppermost ~100 nm of grain surfaces directly exposed to interplanetary space [1]. Laboratory ion irradiation experiments and numerical models predict that ion-damaged rims in olivine should be completely amorphous after receiving irradiation fluences on the order of 10^{16} ions/cm^2 [2-3]. However, lunar and Itokawa olivine grains that experienced exposure timescales exceeding this critical amorphization fluence exhibit *nanocrystalline* rather than completely amorphous rims, with high-defect densities and very few to no localized regions of amorphous material [5-7]. The lack of complete amorphization in lunar and Itokawa olivine particles is even more perplexing considering other mineral phases returned from the same parent bodies, such as plagioclase, have completely amorphous rims of uniform and predictable thickness [5-7].

One possible explanation for the microstructural discrepancy between experimentally ion irradiated and solar wind irradiated olivine is the difference in incident ion flux. For planetary bodies ≥ 1 A.U., solar wind typically has an ion flux ~4-5 orders of magnitude lower than experimental conditions (10^{12}-10^{13} ions/cm^2/s) [4,8-9]. The lower flux of solar wind may ensure that the rate of point defect accumulation is slow enough that olivine grains are able to crystallographically recover through dynamic diffusion processes [3].

With the recent return of samples from asteroid Ryugu by JAXA's Haybusa2 mission and the forthcoming return of samples from asteroid Bennu by NASA's OSIRIS-REx mission, it is imperative to understand how ion flux influences amorphization of the various silicate phases common to carbonaceous asteroidal regolith. Here, we present results from low flux H^{+} and He^+ ion irradiation experiments performed on the Murchison (CM2) carbonaceous chondrite.

Methods: Under ultra-high vacuum (10^{-8} Pa), we irradiated ~10 mm x 10 mm regions of two dry-cut Murchison slices with 1 keV H^+ and 4 keV He^+, respectively. The H^+-irradiation experiment used a flux of 6.6 x 10^{11} ions/cm^2/s and reached a total fluence of 3.9 x 10^{16} ions/cm^2 (~30 years at Bennu). The He^+-irradiation experiment used a flux of 3.6 x 10^{11} ions/cm^2/s and reached a total fluence of 2.1 x 10^{16} ions/cm^2 (~400 years at Bennu). These fluxes, which are ~2 orders of magnitude lower than the fluxes used in our previous Murchison ion irradiation experiments [8], are closer to the ~10^8 ions/cm^2/s flux of solar wind.

Detailed characterizations of the unirradiated, H^+-irradiated, and He^+-irradiated surfaces were performed using a suite of coordinated analytical techniques. *In-situ* X-ray photoelectron spectroscopy (XPS) data acquired with the PHI Versaprobe III Scanning XPS (AlKα: 1486.7 eV) were used to evaluate changes in sample surface chemistry driven by irradiation. Changes in spectral slope, albedo, and absorption band strength were identified using visible to near-infrared (VNIR; 0.35 - 2.5 µm) spectra collected with a fiber-optic ASD FieldSpec 3 Hi-Res Spectroradiometer under ambient laboratory conditions. Finally, the microstructure and composition of focused ion beam cross-sections (FIB-sections) extracted from matrix material and olivine in the H^+- and He^+-irradiated samples were examined using an FEI Talos 200X scanning transmission electron microscope (STEM) equipped with a Super-X energy dispersive X-ray spectroscopy (EDS) detector.

XPS Analysis: All points analyzed with XPS have similar starting chemistries consisting of C, O, Na, Mg, Al, Si, S, Cl, Ar, Ca, Fe, and/or Ni. He^+-irradiation decreases carbon content in the outermost ~10 nm of the sample by ~4.9-8.5 at.%. H^+-irradiation also reduces surface carbon abundance, but to a lesser extent (~2.3-3.8 at.%). High-resolution spectra of the Fe2p region demonstrate peak shifts towards lower binding energy with progressive H^+- and He^+-irradiation. Both types of ion irradiation reduce Fe^{3+} to Fe^{2+}, but no Fe^0 is observed at final fluences (~10^{16} ions/cm^2) (Fig. 1). Analysis of the C1s and S2p regions indicate that H^+- and He^+-irradiation preferentially remove or reduce oxygenated carbon species to polycyclic C-H/C-C species and surface sulfates to native sulfides.

VNIR Analysis: Compared to the unirradiated

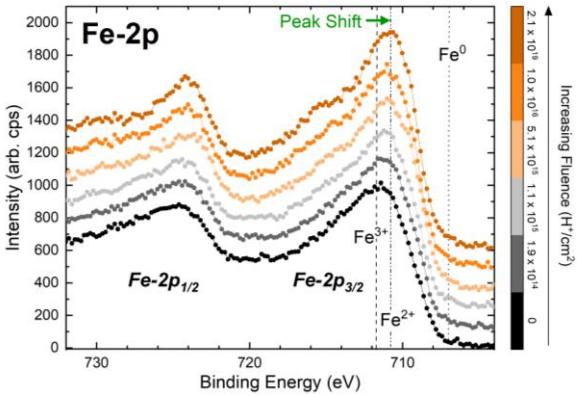

Figure 1. *High-resolution XPS spectra in the Fe2p region acquired from H^+-irradiated matrix material.*

Murchison spectrum from [8], the low flux H^+- and He^+-irradiated absolute reflectance spectra are brighter at all wavelengths (Fig. 2). The H^+-irradiated spectrum exhibits greater brightening and a slightly bluer (i.e., more negative) slope over 0.65-2.5 µm than the He^+-irradiated and unirradiated spectra. All continuum-removed reflectance spectra show a broad band between ~0.6-1.6 µm. The general shape of this band is similar in the unirradiated and He^+-irradiated spectra, with band minima at wavelengths consistent with mixed-valence state serpentines (at ~0.75, 0.95, and 1.15 µm) [10]. The broad band of the H^+-irradiated spectrum consists of only two minima: a stronger, broad absorption centered at ~0.86 µm and a weaker absorption at 1.15 µm.

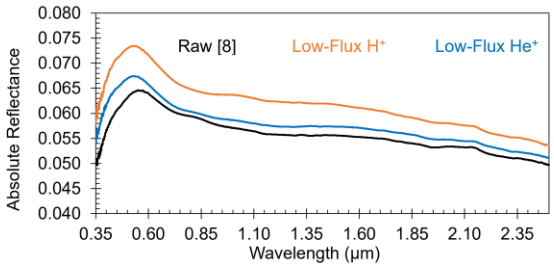

Figure 2. *Absolute reflectance spectra of unirradiated [8], H^+-irradiated, and He^+-irradiated Murchison.*

TEM/EDS Analysis: Unlike matrix FIB-sections analyzed in our high flux study [8], TEM images of this study's He^+-irradiated matrix FIB-section show no distinct ion-affected layer at the surface (Fig. 3a). Vesicles were not identified in this layer and no change in elemental composition with depth was observed in EDS maps. The surface of the He^+-irradiated olivine FIB-section exhibits a continuous, microstructurally-damaged ion-affected layer that varies between ~60-80 nm in thickness and lacks vesicles (Fig. 3b). EDS analysis and high-resolution TEM imaging of these He^+-irradiated FIB-sections will constrain the compositional variation and degree of crystallinity at the near-surface. Analysis of FIB-sections from the low flux H^+-irradiation experiment is ongoing.

Discussion: Results presented here may provide *preliminary* evidence that lower flux ion irradiation alters chemistry and microstructure differently than higher flux experiments using similar ions and energies. Compared to high flux experiments [8] which showed minor chemical reduction of Fe to its metallic state, this work suggests that low flux H^+- and He^+-irradiation may not reduce native Fe^{3+} and Fe^{2+} to Fe^0. However, it must be noted that our samples were irradiated to lower total fluences than samples from [8]—a difference which may also contribute to the absence of chemically reduced Fe^0. Spectral brightening may reflect changes in organic functional group chemistry, removal of surface carbon, or an increase in nanometer-scale surface roughness derived from ion irradiation [9-12]. Considering XPS data shows a more significant decrease in carbon content in the He^+-irradiated sample, removal of surface carbon alone cannot explain the greater spectral brightening of the H^+-irradiated VNIR spectrum. Alternatively, variation in VNIR spectra may reflect intrinsic differences in starting composition of the Murchison samples rather than irradiation processes (e.g., different proportions of chondrules vs. matrix).

TEM results may suggest that ion flux impacts the extent of damage in olivine and matrix material, although additional experiments constraining the critical amorphization and vesiculation fluences of phyllosilicate-bearing matrix are needed. High flux irradiated FIB-sections analyzed by [8] all contained vesicles within their ion-affected surface layers. However, vesicles have not been identified in the low flux He^+-irradiated matrix and olivine FIB-sections presented here. Interestingly, vesicles were observed in olivine samples from [2] and [13] which were irradiated to fluences similar to the final fluences achieved in this study's experiments. This finding may indicate that the low ion flux of solar wind contributes to the paucity of vesicles in space weathered rims of lunar and Itokawa regolith grains compared to experimental samples [4,5-7,14]. Continuing to quantify how different *fluxes and fluences* alter the microstructure and composition of various silicate phases is pertinent to the development of models that predict exposure timescales of returned samples and space weathering rates on airless bodies.

References: [1] Pieters C.M. & Noble S.K. (2016) *JGR 121*(10), 1865-1884 [2] Carrez P. et al. (2002) *MaPS 37*, 1599-1614 [3] Keller L.P. et al. (2021) *MaPS* 56(9), 1685-1707 [4] Keller L.P. & McKay D.S. (1997) *GCA 61*, 2331-2341 [5] Keller L.P. & Berger E.L. (2014) *EPS 66*, 71 [6] Noguchi T. et al. (2014) *MaPS 49*(2), 188-214 [7] Thompson M.S. et al. (2014) *EPS 66*, 89 [8] Laczniak D.L. et al. (2021) *Icarus 364*, 114479 [9] Moroz L. et al. (2004) *Icarus 170*, 214-228 [10] Cloutis, E.A. et al. (2011) *Icarus 216*, 309-346 [11] Dukes C.A. et al. (2015) *SpW Workshop*, #2063 [12] Thompson M.S. et al. (2020) *Icarus 346*, 113775 [13] Thompson M.S. et al. (2019) *LPSC L*, #1425 [14] Matsumoto T. et al. (2015) *Icarus 257*, 230-238

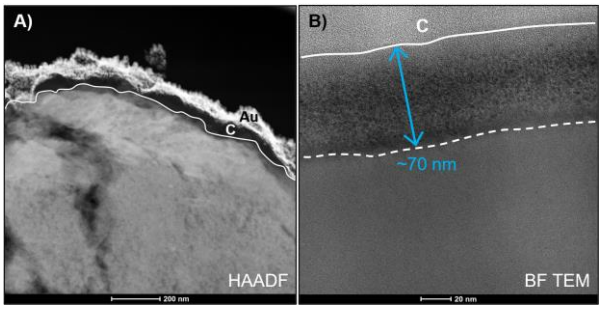

Figure 3. *(A) HAADF STEM image of the He^+-irradiated matrix FIB-section. (B) BF TEM image of the He^+-irradiated olivine FIB-section. Blue arrow shows the thickness of the ion irradiated region.*